

# We are IntechOpen, the world's leading publisher of Open Access books Built by scientists, for scientists

**4,800**

Open access books available

**122,000**

International authors and editors

**135M**

Downloads

Our authors are among the

**154**

Countries delivered to

**TOP 1%**

most cited scientists

**12.2%**

Contributors from top 500 universities



**WEB OF SCIENCE™**

Selection of our books indexed in the Book Citation Index  
in Web of Science™ Core Collection (BKCI)

Interested in publishing with us?  
Contact [book.department@intechopen.com](mailto:book.department@intechopen.com)

Numbers displayed above are based on latest data collected.

For more information visit [www.intechopen.com](http://www.intechopen.com)



# Virtual PET Scanner – From Simulation in GATE to a Final Multiring Albira PET/SPECT/CT Camera

M. Balcerzyk<sup>1,5</sup>, L. Caballero<sup>3</sup>, C. Correcher<sup>3</sup>,  
A. Gonzalez<sup>2,3</sup>, C. Vazquez<sup>4</sup>, J.L. Rubio<sup>4</sup>, G. Kontaxakis<sup>4</sup>,  
M.A. Pozo<sup>5</sup> and J.M. Benlloch<sup>2</sup>

<sup>1</sup>National Accelerators Center, University of Seville

<sup>2</sup>I3M, CSIC, Valencia

<sup>3</sup>Oncovision, Valencia

<sup>4</sup>Technical University of Madrid

<sup>5</sup>Complutense University of Madrid  
Spain

## 1. Introduction

Simulation of the Positron Emission Tomography (PET) camera became a useful tool at the level of scanner design. One of the most versatile methods with several packages available is Monte-Carlo method, reviewed in (Rogers 2006). It was applied in GEANT4 code (Agostinelli *et al.* 2003) used in nuclear physics applications. Other codes used in medical physics and medicine are EGS (for review see (Rogers 2006)), FLUKA (Andersen *et al.* 2005), MCNP (Forster *et al.* 2004), PENELOPE (Sempau *et al.* 2001).

The simulations of PET scanners are done in GATE software (Jan *et al.* 2004) which extensively uses GEANT4. This versatile package offers the possibility of simulation of radioactive source decays. It allows tracking of the individual  $\gamma$  events resulting after positron-electron annihilation. They can be absorbed by photoelectric event in the detector crystal or scattered in the phantom. It allows also simulation of detector electronics including paralyzed mode of the amplifiers. Coincidences can be monitored if they are true or random. The software is now available in version 6.1. Part of the simulations were performed in version 3.0, part in vGate 1.0 (containing version 6.0 via virtualization software for Linux).

GATE was used in simulation of SPECT and CT systems (see papers citing (Jan *et al.* 2004)). Among PET systems for example Siemens PET/CT Biograph 6 scanner (Gonias *et al.* 2007), GE Advance/Discovery LS (Schmidtlein *et al.* 2006), Philips Gemini/Allegro (Lamare *et al.* 2006), Philips Mosaic small animal PET (Merheb, Petegnief and Talbot 2007) or purely *in-silicon* (van der Laan *et al.* 2007) were used for simulation or design of new detectors and systems.

After the initial electronic designs of the camera, its geometry and number of detectors, one can successfully simulate the data collection process including a wide variety of radioactive sources. Data can be classified to individual interactions in the detector (photoelectrically absorbed, scattered), at the coincidence level (true coincidences, scattered coincidences or random coincidences). Singles and coincidences are processed in digitizer module which simulates event collection from initial gamma absorption, via photon generation and reflection within the crystal (not implemented in current simulation), electronic pulse formation, amplification with dead times of the amplifiers, forming of singles and coincidences and then reconstructed into an image of the measured source.

We started from simulating an existing PET scanner called Albira with one ring formed by eight detectors and compared with actual measurements of point sources, animal NEMA phantoms and source grids. As the simulations reproduced very well the actual data in terms of coincidence and single rates, and also in terms of image quality, we moved forward to two and three rings scanner composition, which were at this time only in the design phase. As the electronic modules were to be the same it was a perfect case for simulation.

In the development of new electronics, the depth of interaction was to be included and, this implementation was also simulated in GATE prior to preparation of electronics. This data allow us to observe how the image quality is influenced by the particular implementation of such correction.

On the base of PET camera design and simulation, the multiring version of a breast PET tomograph (MAMMI) was also introduced into the simulation. Again, the simulated data were the base of design modifications and allowed to prepare a reconstruction software long before first real data were taken with a prototype.

## 2. Methods

We thoroughly modified the simulation of 1-ring Albira scanner prepared by Aurora Gonzalez for her Master thesis on the base of the benchmark of a PET scanner simulation included in Gate release (Gonzalez 2008).

Generally, the simulation of the PET scanner contains the following modules and submodules:

1. *Main module*, containing calls to submodules.
2. *Visualization module*, which defines the way the simulation, is presented during run.
3. *Camera module*, which defines tomograph size, crystal dimensions and grouping.
4. *Phantom module*, which defines phantom inserted in the scanner. The phantom can be a geometrical structure or a pixelated phantom, based on 3D image.
5. *Physics module*, which defines the processes to be included in the simulation.
6. *Digitizer module*, which defines how the  $\gamma$  particle detection is processed. It can be very detailed, i.e. storing information on individual interactions in stopping process, then how photons of the scintillation process are reflected in the crystal, how they are detected by the photomultiplier. Then the amplification stage is simulated with energy windows, dead times of the amplifiers, if they are paralyzable or not, etc. This

leads to detection of a single event, which can also be stored, and then processed in several coincidence processors, with individual energy (or signal height) windows, and delays.

7. *Sources module*, which defines sources in geometrical or point form. Sources may be also masked with the phantoms, which allow more complicated geometries, like Derenzo phantom, animal pixelated phantoms, etc.

The listing of the Gate macro with corresponding submodules is provided in Appendix 1 (Section 9.1) of this chapter. The macro is based on benchmarkPET.mac macro provided with Gate 3.0.0. Additional materials used in Gate (in a form readable by Gate) are provided in Appendix 2 (Section 9.2). The file used in Root program (bundled with Gate) to calculate list mode files and statistics can be obtained from the corresponding author (MB, see Appendix 3, Section 10.3)). This program is based on benchmarkPET.C provided with Gate 3.0.0.

The Albira camera mounts one to three rings formed by eight detectors, each containing only one single crystal fit to a position sensitive photomultiplier (PSPMT). One can see the details in Fig.1, Fig.2 and Fig.7. Such large crystal coupled to the PSPMT allows one to additionally detect the depth of interaction of the annihilation gamma ray in the crystal (Lerche *et al.* 2005; Lerche 2006). The position detection resolution in this continuous crystals are  $1.9 \pm 0.1$  mm in plane of the PSPMT (i.e. axial and tangential directions), and about  $3.9 \pm 1.5$  mm in depth direction (i.e. radial). The errors of these values resulted from variation of these values in the crystal space. The largest errors appear in the edges and corners whereas and smallest errors are located in the center of the crystal, as expected.

General characteristics of the simulated Albira camera are as follows:

- 8 tapered center-pointing trapezoid crystals of 9.8 mm thickness (1-ring scanner), or 12 mm thickness (2- and 3-ring scanner).
- Albira crystals are made of LYSO ( $\text{Lu}_{0.95}\text{Y}_{0.05}\text{SiO}_5:\text{Ce}$ )
- The process and stored area of each detector is  $40 \times 40$  mm.
- Dead time for singles is  $0.4 \mu\text{s}$  paralyzable and then  $2 \mu\text{s}$  in non-paralyzable mode, for coincidences is  $1.8 \mu\text{s}$  non-paralyzable mode.
- For simulations we used a mouse phantom and a point-like source at the center of the FOV according to NEMA standard.
- The separation of multiple rings is 4.4 mm. Crystal separation (bore) along the scanner diameter is 112 mm.
- For verification of the 1 ring simulation we placed the “real” mouse phantom in the center of the FOV of the actual scanner and loaded the tube with  $237 \mu\text{Ci}$  of 18-FDG. For a point source measurement, an eppendorf with a droplet of a few tens of  $\mu\text{l}$  (18-FDG) was centered placed. The measurements were performed for about 16 hours to end up at the activities of around  $1 \mu\text{Ci}$ , as suggested also in NEMA standards.
- Radioactivity of  $^{176}\text{Lu}$  was not included in the simulations. In the crystals of Albira we estimate the abundance of  $^{176}\text{Lu}$  (2.59% naturally,  $3.78 \times 10^{10}$  years half-life) to be 280Bq/ml (Moszynski *et al.* 2000).

The sketch of 2-ring scanner is shown in Fig.1

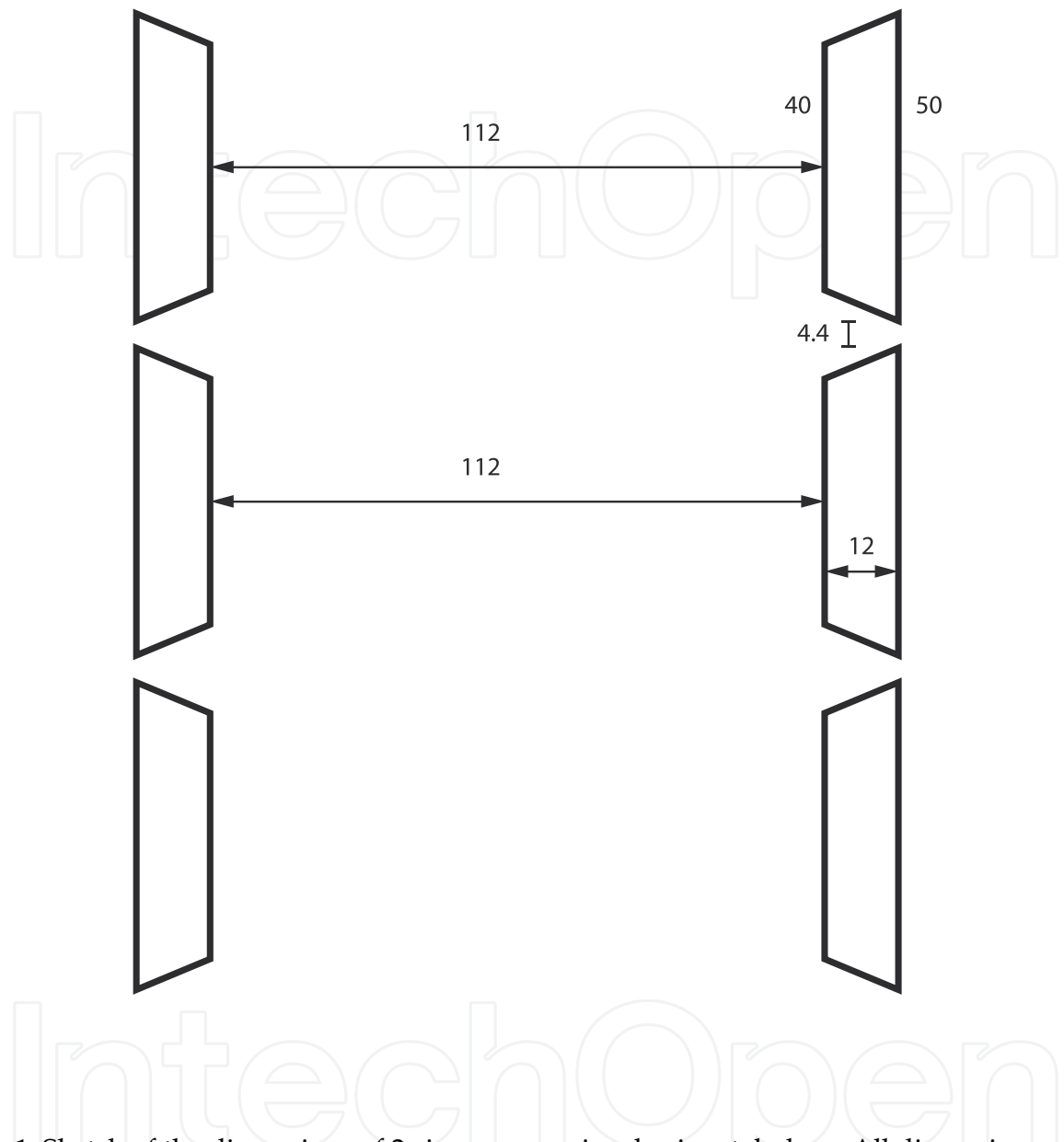


Fig. 1. Sketch of the dimensions of 2-rings camera in a horizontal plane. All dimensions are in mm. For 1-ring scanner the main difference is that the crystals are 9.8 mm thick, instead of 12 mm for 2- and 3-ring scanner. In simulations, 12 mm crystals were used, in actual production they are of 10 mm.

### 3. Validation of simulation for a one-ring scanner with the measurement of mouse phantom

We simulated six different activities for a mouse phantom, exactly the ones that were measured with the phantom. A view of scanner with the mouse phantom and source during the simulation is depicted in Fig.2.

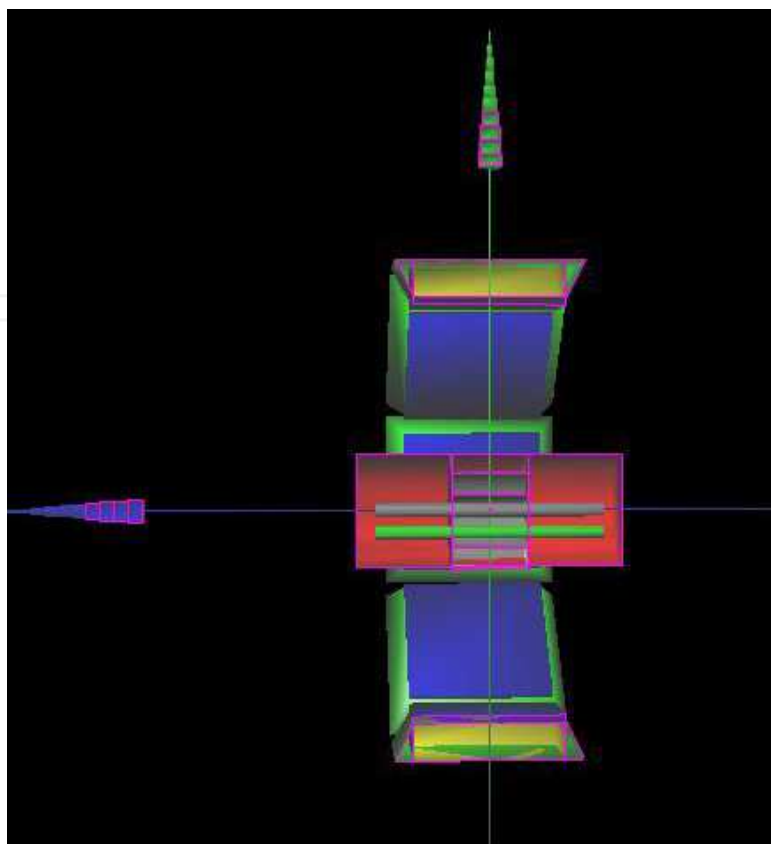


Fig. 2. Simulated 1-ring Albira scanner at a cross section at  $x=0$  plane. XYZ axes are coded as  $x$  in red (not seen in the image),  $y$  in green and  $z$  in blue. The green cylinder in the image represents the location of the tube with radioactive material. In the camera, green structures refer to the crystals.

The simulations were initially done for 1 s acquisition, while the measurements were taken in 10 s frames, and the values of singles and coincidences were counted with a customized Albira application. The comparison between the simulated and acquired real data is shown in Fig.3 and Table 1.

One can see from Fig.3, that coincidence rate is particularly well reproduced almost in the whole activity range down to  $1.5 \mu\text{Ci}$  (-10% error) and reduces to about 20% below  $1 \mu\text{Ci}$  levels.. Single rates are well reproduced down to  $100 \mu\text{Ci}$ , while below this activity the correspondence is quite poor. We would not underestimate the discrepancies for low activities, as this may be the source of artifacts in the images in animals in the areas of low injected activity.

One possible explanation of the effect is the background activity of  $^{176}\text{Lu}$ . The estimate gives the rate of  $^{176}\text{Lu}$  decay events of about 270 cps per ccm, which translates into about 45 kcps in all detectors, and about 2700 cps in one detector at  $\pm 30\%$  energy window (see background spectrum of LSO:Ce in Figure 1 of (Moszynski et al. 2000). 1 ring Albira scanner has 33% solid angle coverage (Balcerzyk et al. 2009).  $0.92 \mu\text{Ci}$  (32 kBq) source generates about 770 singles in a detector. If, as calculated,  $^{176}\text{Lu}$  background is about 2700 cps in a single crystal, we would simulate only about  $770/(770 + 2700) = 22\%$  which corresponds well with 29% shown in Fig.3.

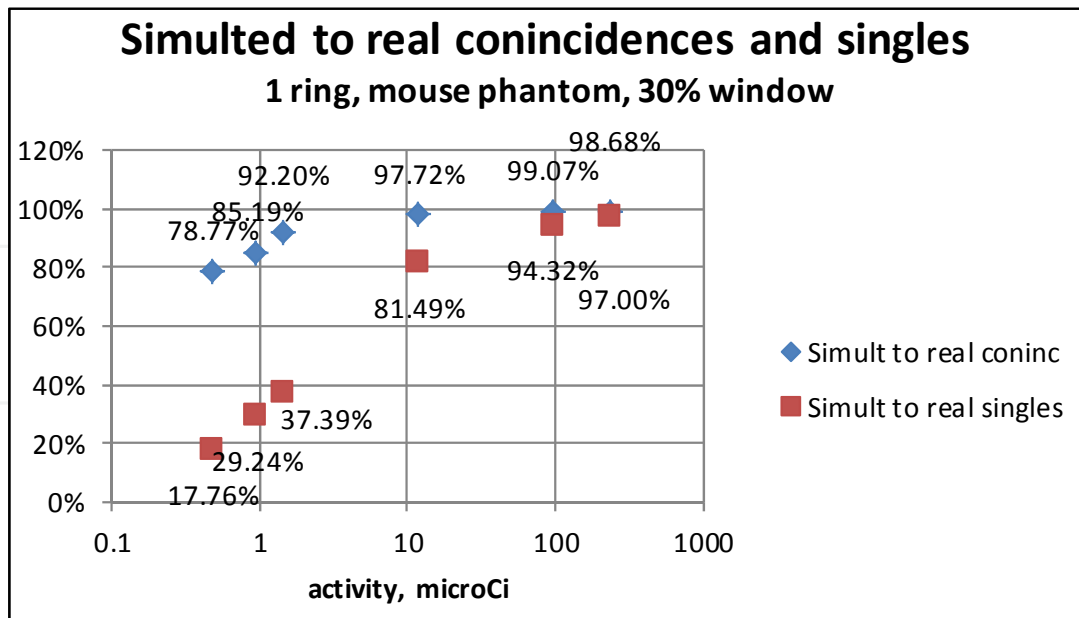


Fig. 3. Comparison between simulated and real coincidences and singles in the 1-ring Albira scanner geometry. Diamonds show the ratio of simulated to real coincidences. Squares show the analogous ratio but for singles. Coincidences are well reproduced (i.e. above 90% agreement) down to 1.5  $\mu\text{Ci}$ , while singles agree well for activity values higher than about 50  $\mu\text{Ci}$ . Data labels indicate detailed values of these ratios.

Activity, kBq	Measured coincidences rate, 1 ring	Measured singles rate, 1 ring	Simulated coincidences rate, 1 ring	Simulated singles rate, 1 ring
8769	30197	901229	26743	835574
7892	28866	845677		
7015	27969	792326		
6138	26603	728288		
5261	24924	652691		
4384	22577	575520		
3507	20024	489651	18068	441574
2630	16700	392602		
1753	12283	280864		
877	6938	156013		
438	3640	87008	3295	67749
263	2266	58374		
175	1549	43782		
88	799	29248		
53	500	23526	431	8414
35	337	19878	267	5552
17	196	16525	141	2799

Table 1. Detailed comparison between single and coincidence rates for 1-ring scanner, used to calculate the diagram in Fig.3 for a mouse phantom. Note that for activities below 1.5  $\mu\text{Ci}$  there is a slight discrepancy between simulated and registered singles.

A 5 ns coincidence window should translate into about 1 to 2 cps in coincidences, which is the measured rate in empty scanner. We see in Table 1 that for all very low activities there is about 50 cps coincidence differences between measured and simulated ones. For the same activities, the singles difference is about 15 kcps, which increases to about 70 kcps for high activities. 15 kcps difference in singles treated as randoms yields about 2.3 cps in coincidences (from  $R=2\tau S^2$  relation,  $R$  being randoms,  $S$  singles rate,  $\tau$  coincidence window (Balcerzyk et al. 2009)).

With the above in mind, one can tell, that background activity of  $^{176}\text{Lu}$  is rather not responsible for discrepancy between simulation and experiment in coincidences but only for singles. One possible reason may be the singles (and hence coincidences) discarded from the tapered region of the crystals. In simulation, the distinction for the localization is very sharp, as we do not simulate photon transport. In real measurement some of the signal from the tapered area may probably leak into the detected area.

Background activity of  $^{176}\text{Lu}$  is now used in Albira scanner for internal tests of detectors upon initialization of the instrument.

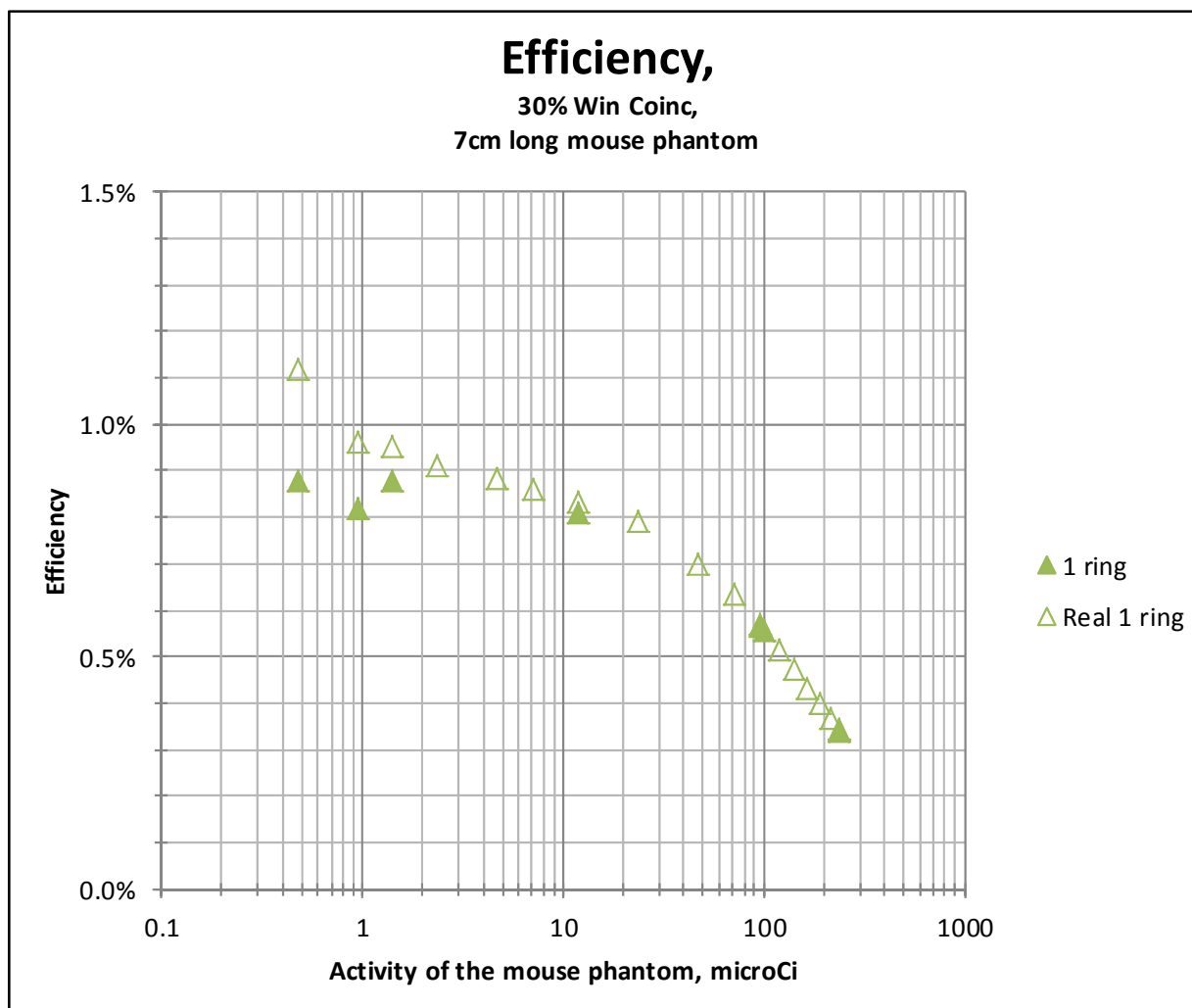


Fig. 4. Efficiency for a mouse phantom simulated (filled symbol) in 1-ring camera compared with measured data (open symbol).



The efficiency for low activities stabilizes at about 0.9% regarding measurement and simulates mouse phantom data. Those activities may serve as a reference for saturation and dead time level calculations. For mouse phantom, an activity of 1  $\mu\text{Ci}$  may be taken as a reference, especially for saturation estimations.

The simulation result of a cylindrical phantom for  $\varnothing 10 \times 10 \text{mm}$  and 3.7 MBq  $^{18}\text{F}$  activity is shown in Fig.5 for a cross section perpendicular to 1 ring scanner axis. One can see that true scattered and random coincidences contribute little to the image quality, as their total level is about 10% at NEC maximum. In Fig.6 one can see the contribution of each coincidence type to NEC.

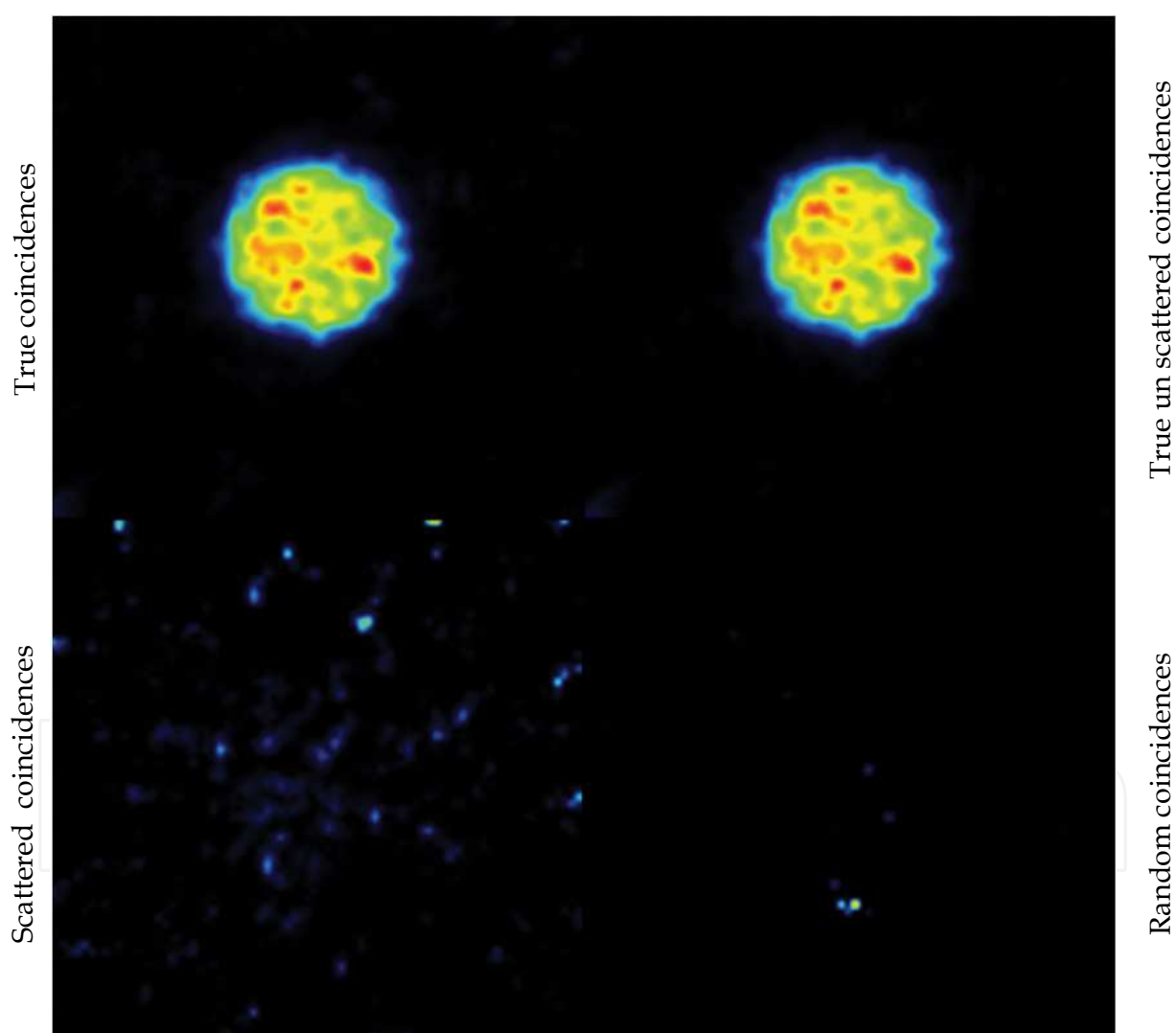


Fig. 5. Gate simulation of  $\varnothing 10 \times 10 \text{mm}$  phantom with a solution of 3.7 MBq of  $^{18}\text{F}$  in water obtained with the 1 ring Albira scanner. Contribution of each type of coincidences is described on the left and right margins. Gate simulated events were converted to four separate list mode files and reconstructed in Albira reconstruction program.

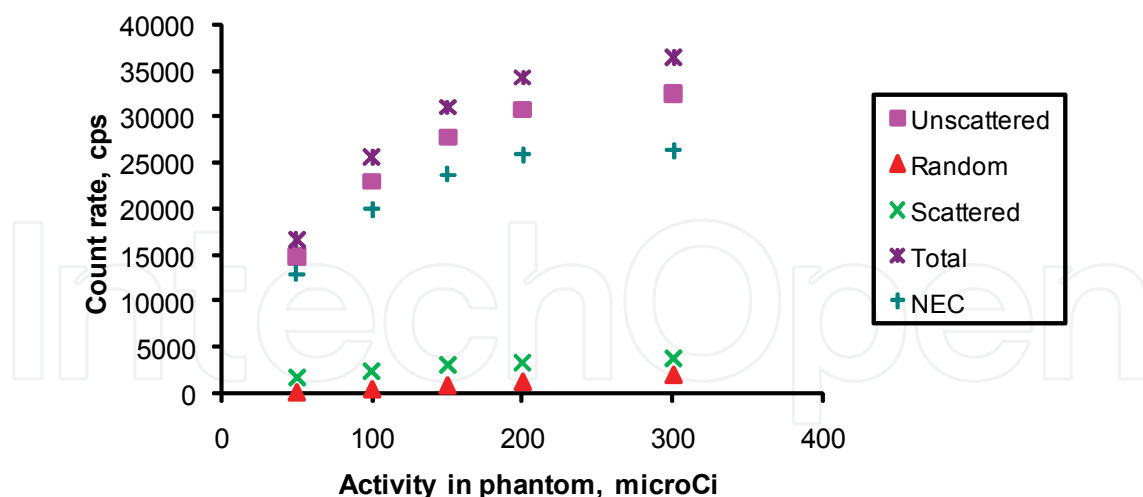


Fig. 6. Simulated NEMA mouse phantom rates for true unscattered, true scattered, random and total coincidences and noise equivalent counts (NEC) for 1 ring Albira scanner. Scatter fraction is constant and about 9% for the whole activity range. NEC has its maximum at 8.8 MBq of the described mouse phantom.

#### 4. Three- and two-ring scanner simulation

The 3D renders of the 2- and 3-ring scanner with the mouse phantom inside the camera are shown in Fig.7.

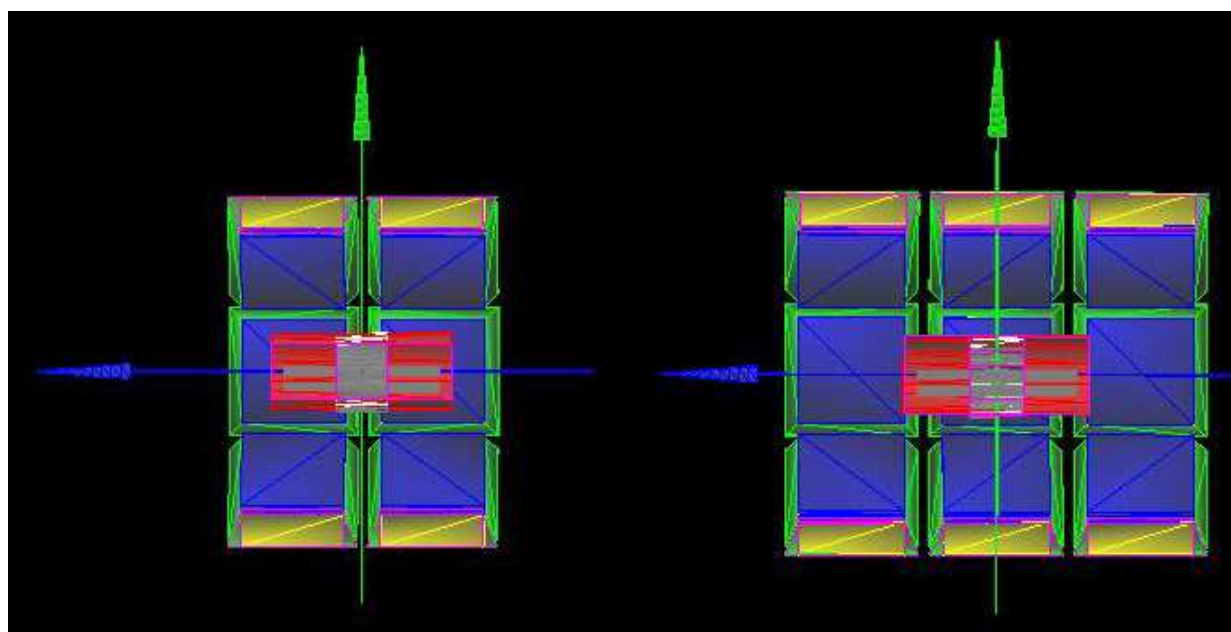


Fig. 7. The cross section view at around  $x=0$  of the simulated 2- and 3-ring scanner with the mouse phantom inside. The coding of the colors is the same as in Fig.2, disregard extra shapes inside the red mouse phantom.

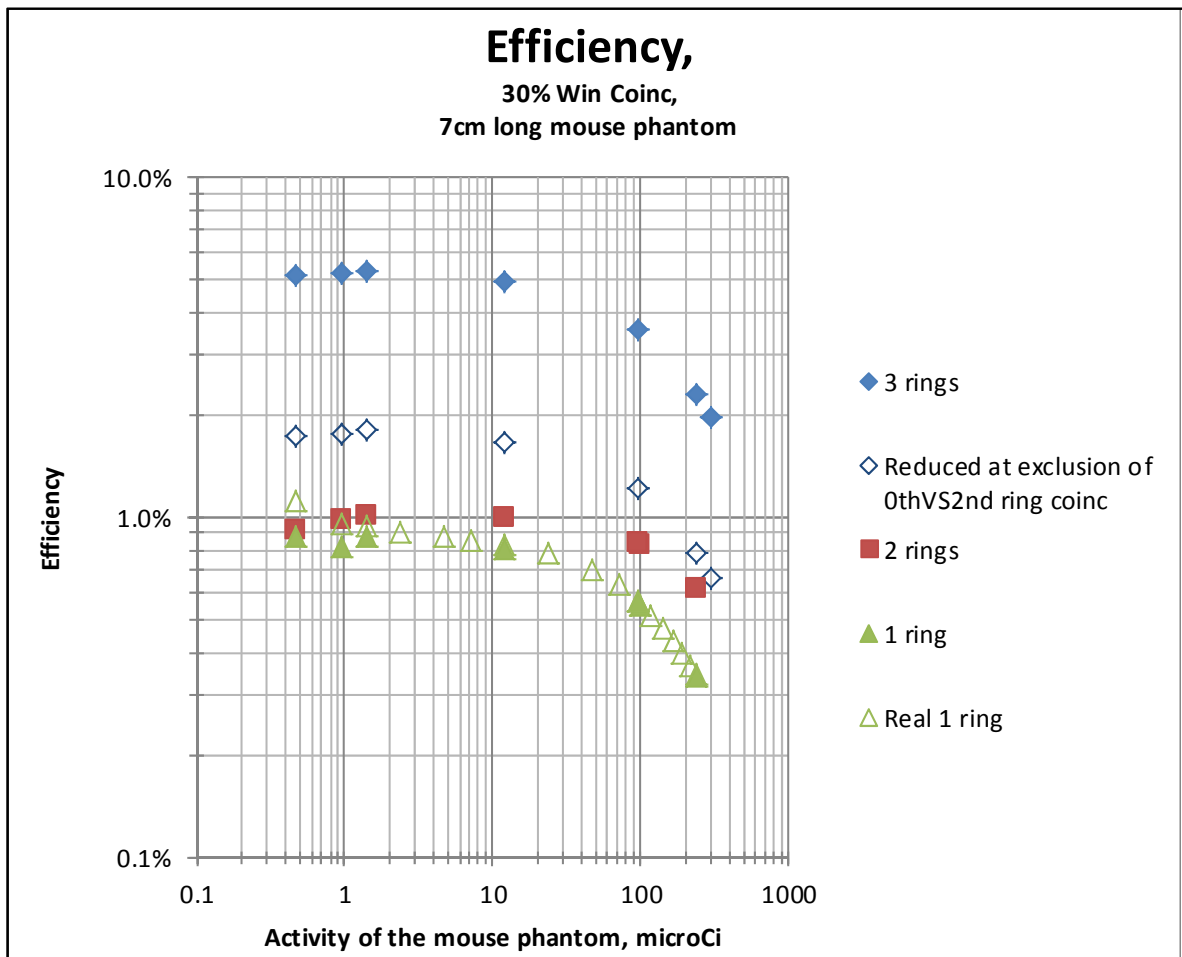


Fig. 8. Efficiency in 30% energy window of coincidences for 1-, 2- and 3-ring scanner. Blue shows 3-ring scanner, squares 2-rings and triangles 1-ring geometry. Open diamonds show the efficiency for a 3-ring scanner with removed coincidences between 0<sup>th</sup> and 2<sup>nd</sup> ring (border rings).

## 5. Efficiency

Fig.8 shows the efficiencies for coincidences for 30% energy window for 1-, 2- and 3-ring scanner for simulations with closed symbols. 1-ring values are the same as in Fig.4. In this picture one can see the power of a 3-ring scanner, where all coincidences are stored. With a mouse phantom the efficiency reaches 5.3% for low activities. Assuming the proper simulation of 1-ring camera, one can expect the same efficiency for a measured mouse phantom, and for real animal measurements.

With open diamonds we show the efficiency in the projected 3-ring scanner with omission of the coincidences between border rings 0<sup>th</sup> and 2<sup>nd</sup>. In one of the first projects, such design was considered. It was estimated by analysis of first 50 coincidences from that scanner for the pair of detectors which form the coincidence. Once can generate such ASCII output in a table from Gate. The coincidences between rings 0<sup>th</sup> and 2<sup>nd</sup> include about 34% of all detected coincidences. The line of response is at small angle towards z-axis of the scanner, so one can expect large parallax errors for this pair of detectors. That effect suggested to include the depth of interaction encoding, which was considered in the final version.

### 5.1 Saturation level

Saturation levels for multiring scanners are shown in Fig.9. They heavily rely on the choice of the two activities for which the efficiency is constant within 5%, being around  $1\mu\text{Ci}$ . However, some simulations there is higher efficiency at  $0.5\mu\text{Ci}$  activity. The difference may be due to fluctuations of small numbers, as the coincidence count for these activities is around a few hundreds. In this only aspect 2-ring scanner is better than 1- and 3-ring scanner. The saturation of 50% for 1- and 3-ring scanner is at the level of about  $120\mu\text{Ci}$ , while for 2-ring scanner it is about  $320\mu\text{Ci}$ . We do not see the reason for 2-ring scanner to behave so well in terms of saturation. It is possible that it is a geometrical effect of having smaller fraction of the phantom within FOV of each ring in this geometry (see Fig.7).

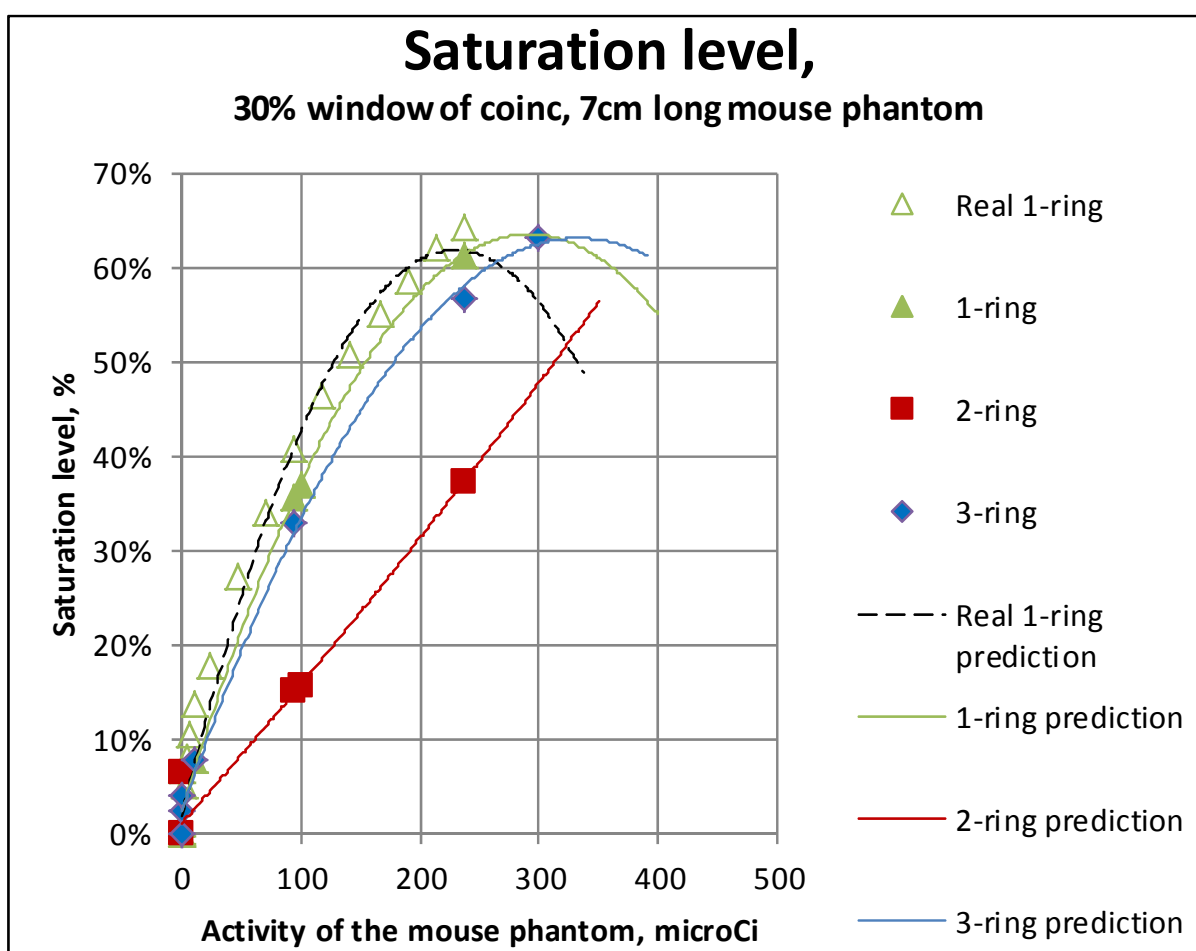


Fig. 9. Saturation levels for multiring scanners. For the 3-ring scanner with omitted 0<sup>th</sup> vs. 2<sup>nd</sup> ring coincidences, the saturation curve would be the same as for 3-ring geometry, as the efficiency is calculated as a fraction of valid coincidences for all activities. As the number of points for simulation is limited, we added the trend lines (2<sup>nd</sup> order polynomials) to look for expected evolution at higher activities.

We drew also prediction lines using simple polynomial 2 curves level. The predictive value of this curve is low, but it shows, that the expected 50% saturation level for 3-ring scanner is higher than for 1-ring scanner.

## 5.2 Omission of 0<sup>th</sup> vs 2<sup>nd</sup> ring coincidences in 3-ring scanner

The reader may have already found that we try to encourage the designers to drop the idea of excluding 0<sup>th</sup> vs. 2<sup>nd</sup> ring coincidences. It would result in the loss of 34% of detected coincidences. In Gate, there is no straightforward way to exclude the mentioned coincidences from the simulation. The only way we perceive it, is to post-hoc exclude them from simulated 3-ring scanner during the creation of list mode files. The problem is that there will be false overestimation of saturation, dead times for coincidences and others during the simulation, so the resulting list mode file will have an artificially lower coincidence level.

## 6. Point source

The proper way (NEMA standard) to measure the efficiency is to place a point source of activity corresponding to saturation level of less than 5% in the center of FOV. The simulations were done for exactly 0.95  $\mu\text{Ci}$  source, which roughly fulfills the requirement and the results are shown in Fig.10 in comparison with the real study in 1-ring scanner. The real scanner measurement was done using a droplet of few tens of  $\mu\text{l}$  of about 10 $\mu\text{Ci}$  of 18-FDG placed in the eppendorf tube and at the center of FOV. For the 1-ring scanner the measured value is 2.49%, while simulation returns 3.2% being in reasonable agreement with expected 10% saturation level at 10  $\mu\text{Ci}$ . Again, one can see the superiority of 3-ring scanner reaching 9.35% efficiency. This value may be further increased to about 12.9% if the tapered areas of the crystal are used for the coincidence detection. This would require most likely sophisticated point-spread function inclusion in the reconstruction besides other technical challenges regarding position calibration of such impinging events.

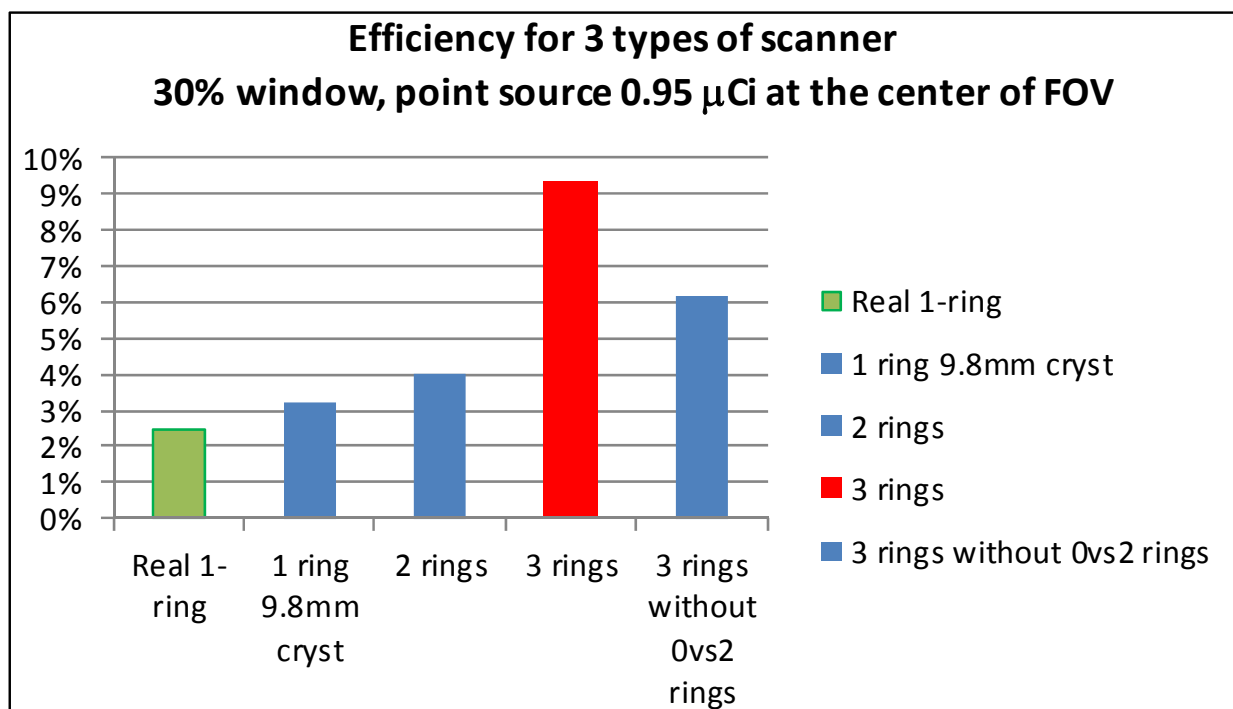


Fig. 10. Efficiency for a real 1-ring scanner and simulated multiring scanners for the low activity (0.95  $\mu\text{Ci}$ ) point source placed in the center of FOV.

## 7. Depth of interaction

For the sources or phantom parts far radially from the center of the field of view, the resolution is deteriorating, mainly due to the so-called parallax error. To correct it, if possible, depth of interaction (DOI) of the detection of annihilation 511 keV  $\gamma$  photon needs to be recorded, and not only planar coordinates in plane of the photomultiplier. In the Albira detector, the DOI is estimated from the scintillation light spread into the position sensitive photomultiplier as shown in Fig.11.

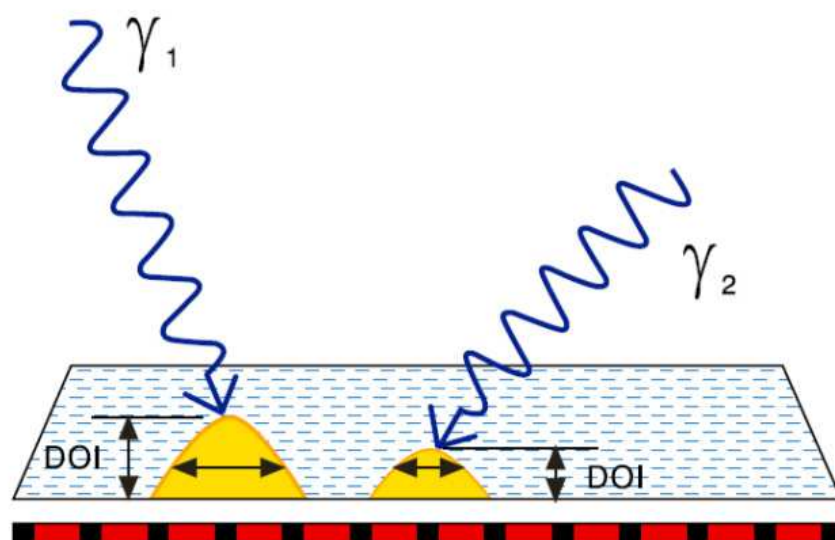


Fig. 11. Scheme of DOI detection in Albira PET detector. From (Oncovision).

In the current Albira 3 ring scanner the DOI is included, but not in the simulations. The DOI is included in the following way: the exact line of response is calculated for each detected coincidence connecting the point corresponding to detected blue arrow in Fig.11 to the interaction point in second detector. The cross section point with the surface optically coupled to the photomultiplier is then re-calculated. This corresponds to already stored LOR for planar detectors. One can see that this sort of DOI for very oblique angles of LOR may result in cross sections with neighboring detectors.

The simulation did not include DOI corrections. The interaction point on the plane of PMT corresponded to the planar simulated coordinates.

## 8. Conclusion

Surprisingly for a point source there is little (from 3% to 4%) increase in efficiency for 2 ring scanner compared to 1-ring (see Fig.10). The larger difference appears with the inclusion of a third ring and, moreover, if coincidences among all rings are allowed, resulting in a efficiency increase up to 9.35%. Higher values reaching 12.9% efficiency would be expected if the events impinging the tapered parts of the crystals are also used for reconstruction.

Upon the simulations results, some managerial decisions in Oncovision have been made. Namely, for 3 ring scanners, coincidences in between all three rings were included in the

final product. Depth of interaction correction was introduced as well. For future versions, inclusion of all coincidences, also from the tapered region of the crystal would be available, as it considerably increases the detector total efficiency.

## 9. Acknowledgements

We thank Aurora Gonzalez for initial adaptation of benchmarkPET.mac macro to one ring Albira scanner.

## 10. Appendices

### 10.1 Appendix 1: Albira macro files listing for 3 ring scanner Gate simulation

Note that that all files must be in one directory. All lines in \*.mac files end with Linux LF end of line character only. In the listing above, long lines are continued in the following one, with the first having hanging indent. Macro is based on benchmarkPET.mac provided with Gate 3.0.0 and Gate 6.0 (Jan et al. 2004).

#### 10.1.1 Main macro

```
# /control/execute *.mac calls the lower level macro
#/vis/disable
/control/execute visu.mac

/gate/geometry/setMaterialDatabase .././GateMaterials.db
# LYSOAlbira and Nylon added

#      W O R L D
/gate/world/geometry/setXLength 150. cm
/gate/world/geometry/setYLength 150. cm
/gate/world/geometry/setZLength 150. cm

/control/execute camera.mac
/control/execute phantom.mac
/control/execute physics.mac

#      I N I T I A L I Z E
/gate/run/initialize

/control/execute digitizer.mac
# digitizer.mac OK, except for deadtimes 1 and 2 for singles, LES and HES for trapezoid
crystalSD

#      S O U R C E
/control/execute sources.mac
#sources.mac OK with A
```

```
#      VERBOSITY
#/gate/verbose Physic  0
#/gate/verbose Cuts    0
#/gate/verbose Actor   0
#/gate/verbose SD      0
#/gate/verbose Actions 0
#/gate/verbose Step    0
#/gate/verbose Error   0
#/gate/verbose Warning 0
#/gate/verbose Output  0
#/gate/verbose Core    0

/run/verbose 0
/event/verbose 0
/tracking/verbose 0

#      OUTPUT
#ASCII output is disabled
/gate/output/ascii/disable
/gate/output/ascii/setOutFileHitsFlag 0
/gate/output/ascii/setOutFileSinglesFlag 0
/gate/output/ascii/setOutFileCoincidencesFlag 0
#/gate/output/ascii/setOutFileDelayFlag 0

/gate/output/root/enable
/gate/output/root/setFileName AlbiraARS
/gate/output/root/setRootHitFlag 0
/gate/output/root/setRootSinglesFlag 0
/gate/output/root/setRootCoincidencesFlag 1
#/gate/output/root/setRootDelayFlag 1

#      RANDOM
#JamesRandom Ranlux64 MersenneTwister
/gate/random/setEngineName Ranlux64
#/gate/random/setEngineSeed default
#/gate/random/setEngineSeed auto
/gate/random/setEngineSeed 123456789
#/gate/random/resetEngineFrom fileName
/gate/random/verbose 1

#      START
/gate/application/setTimeSlice 1. s
/gate/application/setTimeStart 0. s
/gate/application/setTimeStop 1. s
#/gate/application/startDAQ
```



# the # sign may be omitted in the above line to run the macro automatically, otherwise, the above line must be introduced manually in Gate to run the simulation.

#exit

### 10.1.2 Visualize macro: Visu.mac

```
# VISUALISATION
# requires OpenGL graphic card
/vis/open OGLSX
/vis/viewer/set/viewpointThetaPhi 25 45
/vis/viewer/zoom 7
/vis/drawVolume
#/vis/viewer/flush
#/tracking/verbose 0
/tracking/storeTrajectory 1
#/vis/scene/add/trajectories
/vis/scene/endOfEventAction accumulate
```

### 10.1.3 Camera description macro: Camera.mac

```
#-----oooooooooooooooooooooooo-----#
#                                     #
# DEFINITION AND DESCRIPTION        #
# OF YOUR PET DEVICE                #
#                                     #
#-----oooooooooooooooooooooooo-----#
```

#insert 3 axes this does not work in vGate 1.0

#/gate/world/daughters/insert 3axes

#

# CYLINDRICAL : The cylindricalPET system is dedicated  
# for PET device !

#

```
/gate/world/daughters/name PETscanner
/gate/world/daughters/insert cylinder
/gate/PETscanner/setMaterial Air
/gate/PETscanner/geometry/setRmax 70 mm
/gate/PETscanner/geometry/setRmin 55.8 mm
/gate/PETscanner/geometry/setHeight 150 mm
/gate/PETscanner/vis/setVisible 0
```

# PETscanner1 is daughter of PETscanner to correctly place the trpd shape

```
/gate/PETscanner/daughters/name PETscanner1
/gate/PETscanner/daughters/insert cylinder
/gate/PETscanner1/setMaterial Air
/gate/PETscanner1/geometry/setRmax 70 mm
/gate/PETscanner1/geometry/setRmin 55.8 mm
```

```
/gate/PETscanner1/geometry/setHeight 150 mm
/gate/PETscanner1/vis/setVisible 0

/gate/PETscanner/daughters/name LYSO
/gate/PETscanner/daughters/insert box
/gate/LYSO/geometry/setXLength 12 mm
/gate/LYSO/geometry/setYLength 40 mm
/gate/LYSO/geometry/setZLength 40 mm
/gate/LYSO/setMaterial LYSOAlbira
/gate/LYSO/vis/setColor yellow
/gate/LYSO/vis/forceWireframe
# we repeat the block 3x lineary
/gate/LYSO/repeaters/insert cubicArray
/gate/LYSO/cubicArray/setRepeatNumberZ 3
/gate/LYSO/cubicArray/setRepeatVector 0.0 0.0 54.4 mm

#
#      TRPD (level1): Trapezoid LYSO (not used for the moment)
#
/gate/PETscanner1/daughters/name trapezoid
/gate/PETscanner1/daughters/insert trpd
/gate/trapezoid/geometry/setX1Length 50 mm
/gate/trapezoid/geometry/setY1Length 50 mm
/gate/trapezoid/geometry/setX2Length 40 mm
/gate/trapezoid/geometry/setY2Length 40 mm
/gate/trapezoid/geometry/setZLength 12 mm
/gate/trapezoid/setMaterial LYSOAlbira
/gate/trapezoid/vis/setColor green
/gate/trapezoid/vis/forceWireframe
/gate/trapezoid/placement/setTranslation 0. 0. 62. mm

#
#      LEVEL3 : in your crystal unit !
# (front end nylon to be a phantom)
# Nylon is missing in GateMaterial.db, add it
#
# FrontPad was a daughter of PETscanner
/gate/world/daughters/name FrontPad
/gate/world/daughters/insert box
/gate/FrontPad/geometry/setXLength 1.9 mm
/gate/FrontPad/geometry/setYLength 40. mm
/gate/FrontPad/geometry/setZLength 40 mm
/gate/FrontPad/placement/setTranslation 54.85 0. 0. mm
/gate/FrontPad/setMaterial Nylon
/gate/FrontPad/vis/setColor blue
/gate/FrontPad/vis/forceWireframe
/gate/FrontPad/repeaters/insert cubicArray
/gate/FrontPad/cubicArray/setRepeatNumberZ 3
```

```

/gate/FrontPad/cubicArray/setRepeatVector 0.0 0.0 54.4 mm
/gate/FrontPad/repeaters/insert ring
/gate/FrontPad/ring/enableAutoRotation
/gate/FrontPad/ring/setRepeatNumber 8

```

```

# REPEAT YOUR BLOCK (TRPD)
# IN YOURSCANNERPET (8 detectores)
# LYSO box is repeated around z axis
/gate/LYSO/repeaters/insert ring
/gate/LYSO/ring/enableAutoRotation
/gate/LYSO/ring/setFirstAngle 270 deg
# the above line sets the first detector at 12 hour
/gate/LYSO/ring/setPoint1 0. 0. 0. mm
/gate/LYSO/ring/setPoint2 0. 0. -1. mm
/gate/LYSO/ring/setRepeatNumber 8

```

```

#trapezoid is repeated around x axis
/gate/trapezoid/repeaters/insert ring
/gate/trapezoid/ring/enableAutoRotation
/gate/trapezoid/ring/setFirstAngle 270 deg
# the above line sets the first detector at 12 hour
/gate/trapezoid/ring/setPoint1 0. 0. 0. mm
/gate/trapezoid/ring/setPoint2 1. 0. 0. mm
/gate/trapezoid/ring/setRepeatNumber 8
/gate/trapezoid/repeaters/insert cubicArray
/gate/trapezoid/cubicArray/setRepeatNumberX 3
/gate/trapezoid/cubicArray/setRepeatVector 54.4 0.0 0.0 mm
/gate/PETscanner1/placement/setRotationAxis 0 1 0
/gate/PETscanner1/placement/setRotationAngle 90 deg

```

```

# ATTACH SYSTEM : definition of your global detector
/gate/systems/PETscanner/level1/attach LYSO
#/gate/systems/PETscanner1/level1/attach trapezoid

```

```

# ATTACH LAYER SD :
# definition of your sensitive detector
# for trapezoid, below SD must be for trapezoid
/gate/LYSO/attachCrystalSD

```

```

# update the view manually
/vis/drawVolume

```

#### 10.1.4 Mouse phantom description macro: Phantom.mac

```

# PHANTOM 1
/gate/world/daughters/name phantom1
/gate/world/daughters/insert cylinder

```

```
/gate/phantom1/geometry/setRmax 15 mm
/gate/phantom1/geometry/setRmin 0. mm
/gate/phantom1/geometry/setHeight 70 mm
/gate/phantom1/setMaterial Polyethylene
/gate/phantom1/vis/setColor red
/gate/phantom1/vis/forceWireframe

# PHANTOM 2
/gate/phantom1/daughters/name phantom2
/gate/phantom1/daughters/insert cylinder
/gate/phantom2/geometry/setRmax 1.75 mm
/gate/phantom2/geometry/setRmin 0. mm
/gate/phantom2/geometry/setHeight 60 mm
/gate/phantom2/placement/setTranslation 0 -5.9 0 mm
/gate/phantom2/setMaterial Plastic
/gate/phantom2/vis/setColor green
/gate/phantom2/vis/forceWireframe

# PHANTOM 3
/gate/phantom2/daughters/name phantom3
/gate/phantom2/daughters/insert cylinder
/gate/phantom3/geometry/setRmax 1.05 mm
/gate/phantom3/geometry/setRmin 0 mm
/gate/phantom3/geometry/setHeight 60 mm
/gate/phantom3/setMaterial Water
/gate/phantom3/vis/setColor green
/gate/phantom3/vis/forceWireframe

# ATTACH PHANTOM SD
/gate/phantom1/attachPhantomSD
/gate/phantom2/attachPhantomSD
/gate/phantom3/attachPhantomSD
/gate/FrontPad/attachPhantomSD
#FrontPad is defined in camera.mac
```

#### 10.1.5 Physical processes description macro: Physics.mac

```
# PHYSICS
#
/gate/physics/addProcess PhotoElectric
/gate/physics/addProcess Compton
/gate/physics/addProcess GammaConversion
/gate/physics/addProcess LowEnergyRayleighScattering

/gate/physics/addProcess ElectronIonisation
/gate/physics/addProcess Bremsstrahlung
/gate/physics/addProcess PositronAnnihilationStd
```

```

/gate/physics/addProcess MultipleScattering e+
/gate/physics/addProcess MultipleScattering e-

/gate/physics/processList Enabled
/gate/physics/processList Initialized
# CUTS
#
#/gate/phantom1/attachPhantomSD
#/gate/phantom2/attachPhantomSD
#/gate/phantom3/attachPhantomSD
#/gate/FrontPad/attachPhantomSD
#FrontPad is defined in camera.mac, phantomN in phantom.mac

# Cuts for particle in phantoms
/gate/physics/Gamma/SetCutInRegion phantom1 1.0 cm
/gate/physics/Electron/SetCutInRegion phantom1 1.0 cm
/gate/physics/Positron/SetCutInRegion phantom1 1.0 cm

/gate/physics/Gamma/SetCutInRegion phantom2 1.0 cm
/gate/physics/Electron/SetCutInRegion phantom2 1.0 cm
/gate/physics/Positron/SetCutInRegion phantom2 1.0 cm

/gate/physics/Gamma/SetCutInRegion phantom3 1.0 cm
/gate/physics/Electron/SetCutInRegion phantom3 1.0 cm
/gate/physics/Positron/SetCutInRegion phantom3 1.0 cm

/gate/physics/Gamma/SetCutInRegion FrontPad 1.0 cm
/gate/physics/Electron/SetCutInRegion FrontPad 1.0 cm
/gate/physics/Positron/SetCutInRegion FrontPad 1.0 cm

```

### 10.1.6 Digitizer description macro: Digitizer.mac

```

# ADDER
/gate/digitizer/Singles/insert adder

# ENERGYBLURRING
/gate/digitizer/Singles/insert blurring
/gate/digitizer/Singles/blurring/setResolution 0.14
/gate/digitizer/Singles/blurring/setEnergyOfReference 511. keV

# DEADTIME
/gate/digitizer/Singles/insert deadtime
/gate/digitizer/Singles/deadtime/setDeadTime 400. ns
/gate/digitizer/Singles/deadtime/setMode paralysable
/gate/digitizer/Singles/deadtime/chooseDTVOLUME LYSO

```

```
/gate/digitizer/Singles/name deadtime2  
/gate/digitizer/Singles/insert deadtime  
/gate/digitizer/Singles/deadtime2/setDeadTime 2000 ns  
/gate/digitizer/Singles/deadtime2/setMode nonparalysable  
/gate/digitizer/Singles/deadtime2/chooseDTVolume LYSO
```

```
# THRESHOLDER
```

```
/gate/digitizer/Singles/insert thresholder  
/gate/digitizer/Singles/thresholder/setThreshold 357.7 keV  
/gate/digitizer/Singles/insert upholder  
/gate/digitizer/Singles/upholder/setUphold 664.3 keV
```

```
# Singles for energy spectrum:
```

```
/gate/digitizer/name LESingles  
/gate/digitizer/insert singleChain  
/gate/digitizer/LESingles/setInputName Hits  
/gate/digitizer/LESingles/insert adder  
/gate/digitizer/LESingles/insert blurring  
/gate/digitizer/LESingles/blurring/setResolution 0.14  
/gate/digitizer/LESingles/blurring/setEnergyOfReference 511. keV  
/gate/digitizer/LESingles/insert deadtime  
/gate/digitizer/LESingles/deadtime/setDeadTime 400. ns  
/gate/digitizer/LESingles/deadtime/setMode paralysable  
/gate/digitizer/LESingles/deadtime/chooseDTVolume LYSO  
/gate/digitizer/LESingles/name deadtime2  
/gate/digitizer/LESingles/insert deadtime  
/gate/digitizer/LESingles/deadtime2/setDeadTime 2000. ns  
/gate/digitizer/LESingles/deadtime2/setMode nonparalysable  
/gate/digitizer/LESingles/deadtime2/chooseDTVolume LYSO  
/gate/digitizer/LESingles/insert thresholder  
/gate/digitizer/LESingles/thresholder/setThreshold 10. keV  
/gate/digitizer/LESingles/insert upholder  
/gate/digitizer/LESingles/upholder/setUphold 664.3 keV
```

```
# Singles for proper +/-20% coincidences to use:
```

```
/gate/digitizer/name HESingles  
/gate/digitizer/insert singleChain  
/gate/digitizer/HESingles/setInputName Hits  
/gate/digitizer/HESingles/insert adder  
/gate/digitizer/HESingles/insert blurring  
/gate/digitizer/HESingles/blurring/setResolution 0.14  
/gate/digitizer/HESingles/blurring/setEnergyOfReference 511. keV  
/gate/digitizer/HESingles/insert deadtime  
/gate/digitizer/HESingles/deadtime/setDeadTime 400. ns  
/gate/digitizer/HESingles/deadtime/setMode paralysable
```

```

/gate/digitizer/HESingles/deadtime/chooseDTVVolume LYSO
/gate/digitizer/HESingles/name deadtime2
/gate/digitizer/HESingles/insert deadtime
/gate/digitizer/HESingles/deadtime2/setDeadTime 2000. ns
/gate/digitizer/HESingles/deadtime2/setMode nonparalysable
/gate/digitizer/HESingles/deadtime2/chooseDTVVolume LYSO
/gate/digitizer/HESingles/insert thresholder
/gate/digitizer/HESingles/thresholder/setThreshold 408.8 keV
/gate/digitizer/HESingles/insert upholder
/gate/digitizer/HESingles/upholder/setUphold 613.2 keV

```

#### # COINCI SORTER

#Check what is the default multiple coincidence sorter policy, that is:

```

/gate/digitizer/Coincidences/MultiplesPolicy takeAllGoods
/gate/digitizer/Coincidences/setWindow 5. ns
/gate/digitizer/Coincidences/minSectorDifference 3

```

```

/gate/digitizer/name Coincidences2
/gate/digitizer/insert coincidenceChain
/gate/digitizer/Coincidences2/addInputName Coincidences
# no or second chain for coinc
/gate/digitizer/Coincidences2/insert deadtime
/gate/digitizer/Coincidences2/deadtime/setDeadTime 1800. ns
/gate/digitizer/Coincidences2/deadtime/setMode nonparalysable
/gate/digitizer/Coincidences2/deadtime/conservesAllEvent true

```

# 20% window of HESingles used to create real coincidences of Albira

```

/gate/digitizer/name HECoincidences
/gate/digitizer/insert coincidenceSorter
/gate/digitizer/HECoincidences/MultiplesPolicy takeAllGoods
/gate/digitizer/HECoincidences/setWindow 5. ns
/gate/digitizer/HECoincidences/minSectorDifference 3
/gate/digitizer/HECoincidences/setInputName HESingles

```

```

/gate/digitizer/name HECoincidences2
/gate/digitizer/insert coincidenceChain
/gate/digitizer/HECoincidences2/addInputName HECoincidences
/gate/digitizer/HECoincidences2/insert deadtime
/gate/digitizer/HECoincidences2/deadtime/setDeadTime 1800. ns
/gate/digitizer/HECoincidences2/deadtime/setMode nonparalysable
/gate/digitizer/HECoincidences2/deadtime/conservesAllEvent true

```

#### 10.1.7 Source file in sources.mac

```

/gate/source/addSource SourceF
/gate/source/SourceF/setActivity 0.0000009467 Ci
/gate/source/SourceF/gps/particle e+

```

```
/gate/source/SourceF/setForcedUnstableFlag true
/gate/source/SourceF/setForcedHalfLife 6586.2 s
/gate/source/SourceF/gps/energytype Fluor18
/gate/source/SourceF/gps/type Volume
/gate/source/SourceF/gps/shape Cylinder
/gate/source/SourceF/gps/radius 1.05 mm
/gate/source/SourceF/gps/halfz 30. mm
/gate/source/SourceF/gps/angtype iso
/gate/source/SourceF/gps/centre 0. -5.9 0. mm
#/gate/source/SourceF/gps/confine phantom2_P
/gate/source/list
```

## 10.2 Appendix 2. Gatematerials.db file additional materials

```
LYSOalbira: d=7.2525 g/cm3; n=4 ; state=Solid
+el: name=Lutetium ; f=0.725820
+el: name=Yttrium ; f=0.031097
+el: name=Silicon; f=0.063166
+el: name=Oxygen; f=0.179918
Nylon: d=1.15 g/cm3; n=4 ; state=Solid
+el: name=Carbon ; f=0.636853
+el: name=Hydrogen ; f=0.097980
+el: name=Oxygen; f=0.141388
+el: name=Nitrogen; f=0.123779
Polyethylene: d=0.96 g/cm3 ; n=2
+el: name=Hydrogen ; n=2
+el: name=Carbon ; n=1
```

## 10.3 Appendix 3: Root program for preparation of list mode files for reconstruction in Albira program

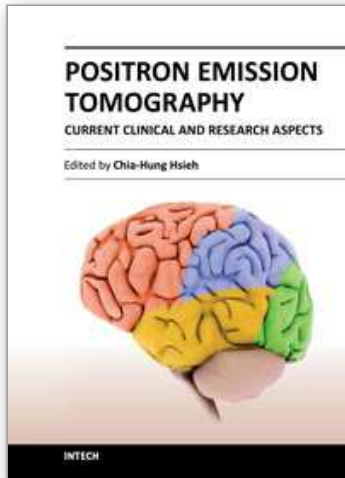
The file can be received from corresponding author (MB) by request. Its size exceeds the allowed size of this publication.

## 11. References

- Agostinelli, S., J. Allison, K. Amako, J. Apostolakis, H. Araujo, P. Arce, et al. (2003). GEANT4 - A simulation toolkit. *Nuclear Instruments and Methods in Physics Research, Section A: Accelerators, Spectrometers, Detectors and Associated Equipment*, Vol. 506, No. 3, pp. 250-303, ISSN 0168-9002
- Andersen, V., F. Ballarini, G. Battistoni, F. Cerutti, A. Empl, A. Fassò, et al. (2005). The application of FLUKA to dosimetry and radiation therapy. *Radiation Protection Dosimetry*, Vol. 116, No. 1-4, pp. 113-117, ISSN 0144-8420
- Balcerzyk, Marcin, George Kontaxakis, Mercedes Delgado, Luis Garcia-Garcia, Carlos Correcher, Antonio J. Gonzalez, et al. (2009). Initial performance evaluation of a high resolution Albira small animal positron emission tomography scanner with monolithic crystals and depth-of-interaction encoding from a user's perspective.



- Measurement Science and Technology*, Vol. 20, No. 10, pp. 104011, ISSN 0957-0233-1361-6501.
- Forster, R. Arthur, Lawrence J. Cox, Richard F. Barrett, Thomas E. Booth, Judith F. Briesmeister, Forrest B. Brown, *et al.* (2004). MCNP™ Version 5. *Nuclear Instruments and Methods in Physics Research Section B: Beam Interactions with Materials and Atoms*, Vol. 213, No. 0, pp. 82-86, ISSN 0168-583X.
- Gonias, P., N. Bertsekas, N. Karakatsanis, G. Saatsakis, A. Gaitanis, D. Nikolopoulos, *et al.* (2007). Validation of a GATE model for the simulation of the Siemens biograph™ 6 PET scanner. *Nuclear Instruments and Methods in Physics Research, Section A: Accelerators, Spectrometers, Detectors and Associated Equipment*, Vol. 571, No. 1-2 SPEC. ISS., pp. 263-266, ISSN 0168-9002
- Gonzalez, A. 2008. M.S. Thesis, Technical University of Madrid, Madrid.
- Jan, S., G. Santin, D. Strul, S. Staelens, K. Assié, D. Autret, *et al.* (2004). GATE: a simulation toolkit for PET and SPECT. *Phys Med Biol*, Vol. 49, No. 19, pp. 4543-4561, ISSN 0031-9155-1361-6560.
- Lamare, F., A. Turzo, Y. Bizais, C. C. L. Rest & D. Visvikis. (2006). Validation of a Monte Carlo simulation of the Philips Allegro/GEMINI PET systems using GATE. *Phys Med Biol*, Vol. 51, No. 4, pp. 943-962, ISSN 0031-9155
- Lerche, C. 2006. Depth of Interaction Enhanced Gamma-Ray Imaging for Medical Applications, Departamento de Física Atomica, Molecular y Nuclear, Universidad de Valencia, Valencia.
- Lerche, C., J. Benlloch, F. Sanchez, N. Pavon, N. Gimenez, M. Fernandez, *et al.* (2005). Depth of interaction detection with enhanced position-sensitive proportional resistor network. *Nucl. Instr. Meth. A*, Vol. 537, No. 1-2, pp. 326-330, ISSN 01689002.
- Merheb, C., Y. Petegnief & J. N. Talbot. (2007). Full modelling of the MOSAIC animal PET system based on the GATE Monte Carlo simulation code. *Phys Med Biol*, Vol. 52, No. 3, (Feb 7) pp. 563-76, ISSN 0031-9155 (Print) 0031-9155 (Linking).
- Moszynski, M., M. Balcerzyk, M. Kapusta, D. Wolski & C. L. Melcher. (2000). Large size LSO:Ce and YSO:Ce scintillators for 50 MeV range  $\gamma$ -ray detector. *IEEE Trans. Nucl. Sci.*, Vol. 47, No. 4, pp. 1324-1328, ISSN 0018-9499.
- Oncovision. 2011. *AlbiraARS brochure* [cited 2011-8-18 2011]. Available from <http://www.gem-imaging.com/descargas/productos/albira.pdf>.
- Rogers, D. W. O. (2006). Fifty years of Monte Carlo simulations for medical physics. *Phys Med Biol*, Vol. 51, No. 13, pp. R287-R301, ISSN 0031-9155
- Schmidtlein, C. R., A. S. Kirov, S. A. Nehmen, Y. E. Erdi, J. L. Humm, H. I. Amols, *et al.* (2006). Validation of GATE Monte Carlo simulations of the GE Advance/Discovery LS PET scanners. *Medical Physics*, Vol. 33, No. 1, pp. 198-208, ISSN 0094-2405
- Sempau, J., A. Sánchez-Reyes, F. Salvat, H. Oulad Ben Tahar, S. B. Jiang & J. M. Fernández-Varea. (2001). Monte Carlo simulation of electron beams from an accelerator head using PENELOPE. *Phys Med Biol*, Vol. 46, No. 4, pp. 1163-1186, ISSN 0031-9155
- van der Laan, D. J., M. C. Maas, H. W. A. M. de Jong, D. R. Schaart, P. Bruyndonckx, C. Lemaître, *et al.* (2007). Simulated performance of a small-animal PET scanner based on monolithic scintillation detectors. *Nucl. Instr. Meth. A*, Vol. 571, No. 1-2, pp. 227-230, ISSN 0168-9002.



## **Positron Emission Tomography - Current Clinical and Research Aspects**

Edited by Dr. Chia-Hung Hsieh

ISBN 978-953-307-824-3

Hard cover, 336 pages

**Publisher** InTech

**Published online** 08, February, 2012

**Published in print edition** February, 2012

This book's stated purpose is to provide a discussion of the technical basis and clinical applications of positron emission tomography (PET), as well as their recent progress in nuclear medicine. It also summarizes current literature about research and clinical science in PET. The book is divided into two broad sections: basic science and clinical science. The basic science section examines PET imaging processing, kinetic modeling, free software, and radiopharmaceuticals. The clinical science section demonstrates various clinical applications and diagnoses. The text is intended not only for scientists, but also for all clinicians seeking recent information regarding PET.

### **How to reference**

In order to correctly reference this scholarly work, feel free to copy and paste the following:

M. Balcerzyk, L. Caballero, C. Correcher, A. Gonzalez, C. Vazquez, J.L. Rubio, G. Kontaxakis, M.A. Pozo and J.M. Benlloch (2012). Virtual PET Scanner – From Simulation in GATE to a Final Multiring Albira PET/SPECT/CT Camera, Positron Emission Tomography - Current Clinical and Research Aspects, Dr. Chia-Hung Hsieh (Ed.), ISBN: 978-953-307-824-3, InTech, Available from:  
<http://www.intechopen.com/books/positron-emission-tomography-current-clinical-and-research-aspects/virtual-pet-scanner-from-simulation-in-gate-to-a-final-multiring-albira-pet-spect-ct-camera>

**INTECH**  
open science | open minds

### **InTech Europe**

University Campus STeP Ri  
Slavka Krautzeka 83/A  
51000 Rijeka, Croatia  
Phone: +385 (51) 770 447  
Fax: +385 (51) 686 166  
[www.intechopen.com](http://www.intechopen.com)

### **InTech China**

Unit 405, Office Block, Hotel Equatorial Shanghai  
No.65, Yan An Road (West), Shanghai, 200040, China  
中国上海市延安西路65号上海国际贵都大饭店办公楼405单元  
Phone: +86-21-62489820  
Fax: +86-21-62489821

© 2012 The Author(s). Licensee IntechOpen. This is an open access article distributed under the terms of the [Creative Commons Attribution 3.0 License](#), which permits unrestricted use, distribution, and reproduction in any medium, provided the original work is properly cited.

IntechOpen

IntechOpen